NEUROSCIENCE

Exercise training improves motor skill learning via selective activation of mTOR

Kai Chen[1], Yuhan Zheng[1], Ji-an Wei[1], Huan Ouyang[1], Xiaodan Huang[1], Feilong Zhang[2], Cora Sau Wan Lai[3,4], Chaoran Ren[1,5,6], Kwok-Fai So[1,4,5,6]*, Li Zhang[1,6]*

Physical exercise improves learning and memory, but little in vivo evidence has been provided to illustrate the molecular mechanisms. Here, we show that chronic treadmill exercise activates the mechanistic target of rapamycin (mTOR) pathway in mouse motor cortex. Both ex vivo and in vivo recordings suggest that mTOR activation leads to potentiated postsynaptic excitation and enhanced neuronal activity of layer 5 pyramidal neurons after exercise, in association with increased oligodendrogenesis and axonal myelination. Exercise training also increases dendritic spine formation and motor learning. Together, exercise activates mTOR pathway, which is necessary for spinogenesis, neuronal activation, and axonal myelination leading to improved motor learning. This model provides new insights for neural network adaptations through exercises and supports the intervention of cognitive deficits using exercise training.

INTRODUCTION

Physical exercise has beneficiary effects on both mental and cognitive functions (*1*–*4*). In particular, acute (*5*, *6*) or chronic aerobic exercises (*7*) improve the acquisition or retention of complex motor skills in humans, in association with enhanced activities of motor-related brain regions (*8*). However, the molecular mechanism for exercise-improved learning remains poorly understood and lacks in vivo evidence. Most of our current knowledge specifies that exercise training enhances the expression of brain-derived neurotrophic factor (BDNF) (*9*–*11*), which can stabilize dendritic spines of mouse barrel cortex for improving the sensory-dependent working memory (*12*). BDNF potentially activates the mechanistic target of rapamycin (mTOR) pathway (*13*), which is crucial for spinogenesis (*14*), axonal regeneration (*15*), and synaptic transmission (*16*). Furthermore, accumulating evidence has demonstrated the activation of mTOR pathway by physical exercise in peripheral tissues (*17*), while its central role is still unclear. The neurobiological study of mTOR pathway thus may help to further elaborate the molecular mechanisms governing exercise-related learning enhancements.

Motor memory can be acquired and stored in the form of cortical spine plasticity (*18*, *19*), and the memory retrieval process is dependent on cortical neuron activities, their connection with other cortical (*20*) or subcortical regions (*21*), in addition to axonal myelination (*22*). Among those cellular processes, long-term treadmill exercise stabilizes dendritic spines of mouse barrel cortex by up-regulating BDNF (*12*). However, the molecular mechanism of exercise training on the neural network is far from complete. We propose that mTOR pathway might be the pivotal intracellular mediator for exercise-enhanced learning functions based on the following reasons: First, the exercise training activates mTOR in various peripheral tissues (*23*) such as skeletal muscles (*24*–*26*). Second, mTOR activation mediates neural network remodeling, including spine plasticity (*14*, *27*, *28*), synaptic transmission (*29*, *30*), and axonal myelination (*31*, *32*). Last, mTOR pathway is necessary for the acquisition and maintenance of memory paradigms, including spatial (*33*, *34*), social (*35*), and motor functions (*36*). Therefore, we hypothesize that exercise activates mTOR to improve learning functions.

After chronic treadmill exercise training, we found that mTOR pathway was activated in mouse motor cortex to potentiate the synaptogenesis. Both ex vivo and in vivo assays showed that exercise training enhanced postsynaptic excitability and neuronal activity of layer 5 pyramidal neuron (L5PRN) in mouse motor cortex and potentiated axonal myelination. Those structural and functional changes are dependent on mTOR activation, as proved by rapamycin inhibition assay. Last, exercised mice presented elevated dendritic spine formation in the motor cortex and enhanced motor learning functions. Together, our findings demonstrate the pivotal role of mTOR in exercise-dependent cortical neural remodeling, which helps to improve the acquisition of motor skills. This model provides new insights for cellular and molecular basis of exercise-induced learning enhancement and further supports the intervention of cognitive deficits by exercise training.

RESULTS

Treadmill exercise training activates mTOR and strengthens postsynaptic densities in mouse motor cortex

We first investigated the molecular pathways after chronic treadmill exercise on mice. Both human studies (*37*) and mouse models (*12*) have demonstrated the involvement of BDNF in cortical reorganization by exercise training. Consistent with those results, matured BDNF and phosphorylated receptor tyrosine kinase B (Trkb) were up-regulated in mouse motor cortex after 21-day treadmill training ($P = 0.0001$ and $P = 0.0398$; Fig. 1, A and B). At the downstream of Trkb, mTOR is known to modulate spine plasticity (*16*). We found elevated phosphorylated levels of mTOR core protein in runner mice ($P = 0.0181$; Fig. 1C), indicating the activation of mTOR by chronic exercise. As further evidence, runner mice also had elevated

[1]Joint International Research Laboratory of CNS Regeneration, Guangdong-Hong Kong-Macau Institute of CNS Regeneration, Jinan University, Guangzhou 510632, P. R. China. [2]Peking University, Drug Discovery Center, Key Laboratory of Chemical Genomics, Peking University Shenzhen Graduate School, Shenzhen 518055, P. R. China. [3]School of Biomedical Sciences, Li Ka Shing Faculty of Medicine, The University of Hong Kong, Hong Kong SAR, P. R. China. [4]State Key Laboratory of Brain and Cognitive Science, Li Ka Shing Faculty of Medicine, The University of Hong Kong, Hong Kong SAR, P. R. China. [5]Co-innovation Center of Neuroregeneration, Nantong University, Jiangsu 226019, P. R. China. [6]Guangzhou Regenerative Medicine and Health Guangdong Laboratory, Guangzhou 510530, P. R. China.
*Corresponding author. Email: hrmaskf@hku.hk (K.-F.S.); zhangli@jnu.edu.cn (L.Z.)

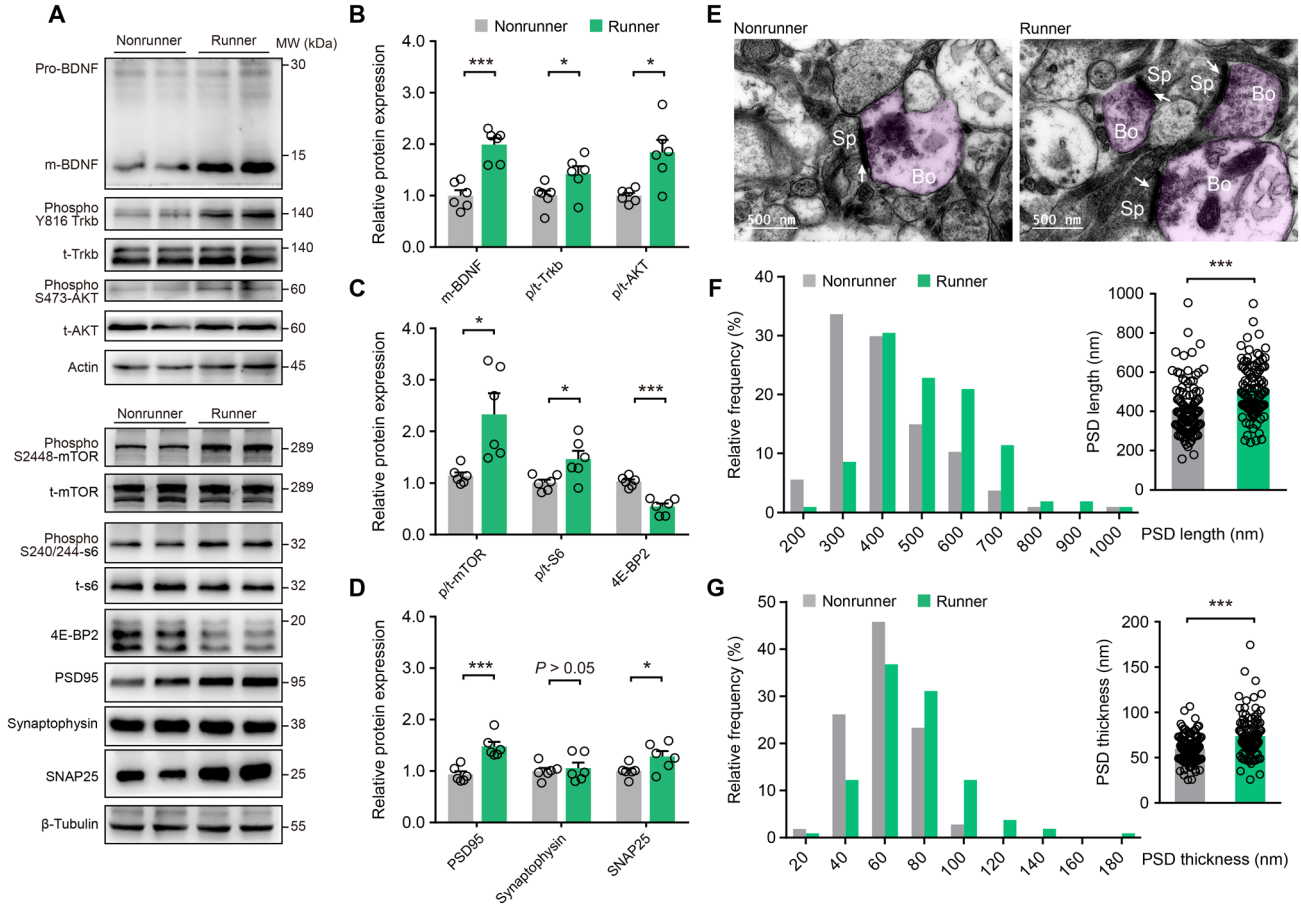

Fig. 1. Long-term exercise activates mTOR and facilitates PSD formation in mouse motor cortex. (**A**) Representative Western blotting bands using total protein extracts from the motor cortex. MW, molecular weight. (**B** to **D**) Quantification of protein expression levels between runner ($n = 6$) or nonrunner ($n = 6$) mice. (B) Exercise elevates matured BDNF (m-BDNF; two-sample student t test, $t_{10} = 7.531$, $P = 0.0001$), phosphorylated/total (p/t) Trkb ($t_{10} = 2.362$, $P = 0.0398$), and phosphorylated/total AKT ($t_{10} = 3.391$, $P = 0.0069$). (C) Phosphorylated/total mTOR protein ($t_{10} = 2.281$, $P = 0.0181$), phosphorylated/total ribosomal S6 protein ($t_{10} = 2.395$, $P = 0.0376$), and inhibited elongation factor 4E-BP2 ($t_{10} = 6.543$, $P < 0.0001$) in exercised mice. (D) Treadmill exercise also elevated postsynaptic protein PSD95 ($t_{10} = 5.012$, $P = 0.0005$) and vesicular protein SNAP25 ($t_{10} = 2.401$, $P = 0.0373$). (**E**) EM images in mouse motor cortex. Bo, axonal bouton; Sp, dendritic spine; white arrows, PSD complex. Scale bar, 500 nm. (**F**) Histogram for the PSD lengths between runners ($n = 105$ synapses from five mice) and nonrunners ($n = 107$ synapses from five mice). Inset: Mean PSD lengths were increased in runner mice ($t_{210} = 5.495$, $P < 0.0001$). (**G**) Histogram for PSD thickness. Inset: Mean PSD thickness were higher in runner group ($t_{210} = 5.133$, $P = 0.0001$). *$P < 0.05$, ***$P < 0.001$. Error bars, SEM.

phosphorylation of ribosomal protein S6 (p-S6; $P = 0.0376$) and suppressed expressions of elongation factor 4E-BP2 ($P < 0.0001$; Fig. 1C). The elevated p-S6 was further validated by the immunohistochemistry staining (fig. S1). These data collectively demonstrated exercise-induced mTOR activation in mouse motor cortex.

The mTOR-S6 pathway facilitates the synthesis of synaptic proteins (*38*) for potentiating synaptic transmissions (*39*). In exercised mice, postsynaptic density of 95 kDa (PSD95) and presynaptic synaptosomal-associated protein 25 (SNAP25) were substantially up-regulated ($P = 0.0005$ and $P = 0.0373$; Fig. 1D). Consistent with those results, both lengths and thicknesses of PSDs in the motor cortex were increased in runner mice by electron microscopy (EM) studies (PSD length, 515 ± 14 nm versus 409 ± 13 nm, $P < 0.0001$; thickness: 73.68 ± 2.25 nm versus 59.82 ± 1.50 nm, $P < 0.0001$; Fig. 1, E to G). Together, chronic treadmill exercise activates the mTOR pathway and enhances synaptogenesis.

Synaptic transmission is potentiated by exercise-induced mTOR activation

Having observed enhanced expressions of synaptic proteins by the exercise training, we next investigated whether the synaptic transmission was also facilitated by performing the whole-cell patch-clamp recording on L5PRN from acute brain slices (Fig. 2, A to C). We chose L5PRN as the recording target due to its role as the major excitatory output of the motor cortex via contralateral and subcortical projections to modulate the motor system and its higher spine plasticity within the apical tuft after motor learning (*19*). Exercise training remarkably elevated the amplitude of miniature excitatory postsynaptic current (mEPSC), and this potentiation was dependent on mTOR activation, as shown by intraperitoneal injection of mTOR inhibitor rapamycin (3 mg/kg body weight, every 3 days) during the 21-day training paradigm (nonrunner + saline, 7.8 ± 0.5 pA; runner + saline, 9.5 ± 0.3 pA; nonrunner + rapamycin, 6.1 ± 0.1 pA; runner + rapamycin, 5.2 ± 0.3 pA; $F_{3,27} = 32.64$, $P < 0.0001$; Fig. 2, D to I). No significant change, however, was found in mEPSC frequencies

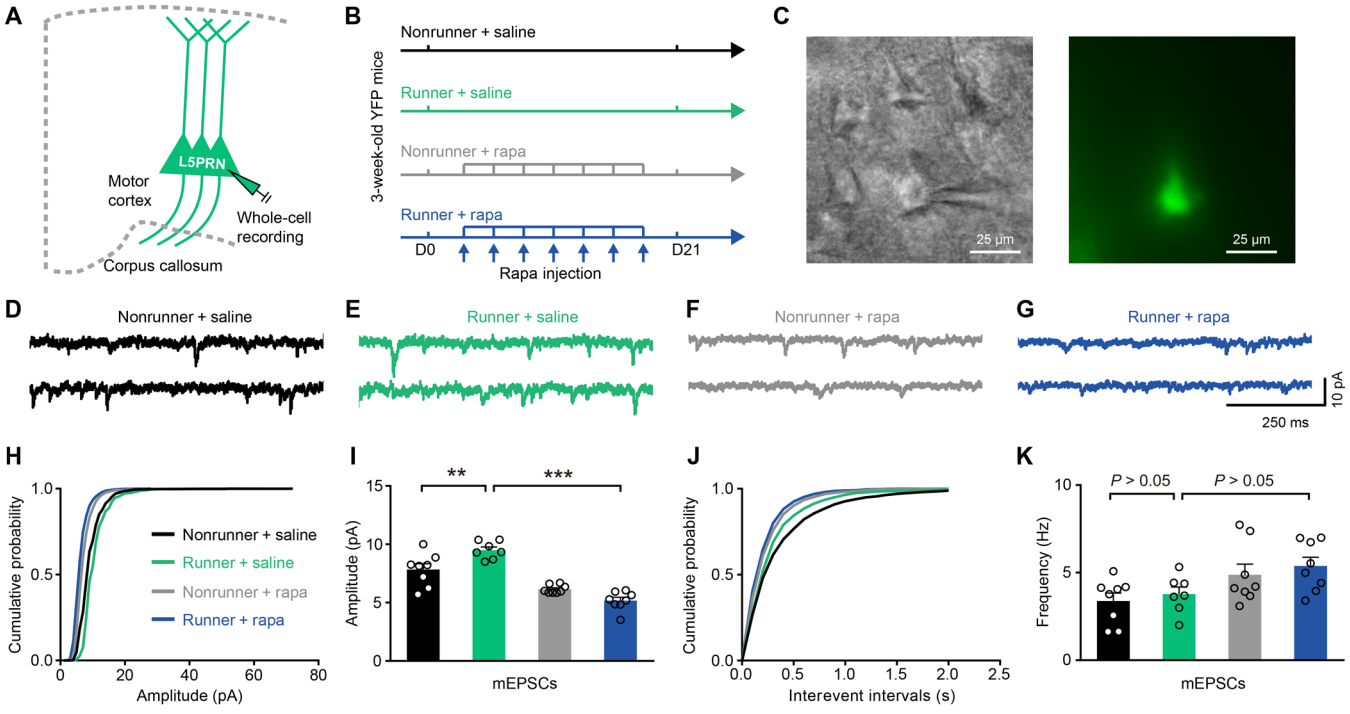

Fig. 2. Exercise training potentiates synaptic transmissions via mTOR activation. (**A**) Illustration for whole-cell recordings of mEPSC of L5PRN in Thy1-YFP mice. (**B**) Schematic diagram for experimental protocols. Rapamycin administration was executed every 3 days during 21-day treadmill training. D0, day 0. (**C**) Bright-field (left) and epifluorescent (right) images of one YFP-labeled L5PRN for the whole-cell recording. (**D** to **G**) From left to right, representative traces of mEPSC extracted from nonrunner + saline ($n = 8$ neurons from four mice), runner + saline ($n = 7$ neurons from three mice), nonrunner + rapamycin ($n = 8$ neurons from four mice), and runner + rapamycin groups ($n = 8$ neurons from three mice). (**H** to **K**) Cumulative distributions of mEPSC amplitudes (H) and mEPSC frequencies (J) were plotted. Quantitative analysis (I and K) showed elevated mEPSC amplitudes in runner mice [one-way analysis of variance (ANOVA), $F_{3,27} = 32.64$, $P < 0.0001$; Tukey post hoc comparison, $q_{27} = 4.966$, $P = 0.0081$ (I)] that was subsequently abolished by rapamycin ($q_{27} = 12.95$, $P < 0.0001$). No significant change was found in mEPSC frequencies [$q_{27} = 0.7616$, $P = 0.9488$ for nonrunner + saline versus runner + saline and $q_{27} = 3.112$, $P = 0.1487$ for runner + saline versus runner + rapamycin (K)]. $^{**}P < 0.01$, $^{***}P < 0.001$. Error bars, SEM.

($P > 0.05$; Fig. 2, J and K). These data seem to indicate potentiated postsynaptic response, rather than enhanced presynaptic vesicle release after exercise. Our rapamycin infusion effectively suppressed mTOR pathway, as suggested by lower p-S6 levels in the motor cortex (fig. S1). The chronic treadmill training thus effectively potentiates synaptic transmissions of L5PRN in the motor cortex via mTOR activation.

mTOR activation is necessary for exercise-enhanced neuron activity in vivo

We further examined whether this exercise-potentiated excitatory postsynaptic transmissions ex vivo can be translated into neuronal activities in vivo. Using immediate early gene c-Fos and Arc as the markers, the activities of pyramidal neurons in both layer II/III and layer V of motor cortex were elevated after 3-week exercise (c-Fos$^+$/CaMKII$^+$, 105 of 376 in nonrunner group and 275 of 423 in runner group, $P < 0.05$; Arc$^+$/CaMKII$^+$, 211 of 215 in runner group only but none in nonrunner group; fig. S2). To provide further in vivo evidences, mice received adeno-associated virus (AAV)–mediated transfection of genetically encoded calcium indicator GCaMP6s into L5PRN of the motor cortex, followed by 21-day treadmill exercise training (Fig. 3, A to C). Using transcranial two-photon imaging on head-fixed awakened mice, we recorded calcium transients of L5PRN from both apical tufts and somas (fig. S3). The peak amplitudes of calcium transients were increased in runner mice (apical dendrites: nonrunner, 2.0 ± 0.1, runner, 3.2 ± 0.2; soma: nonrunner + saline, 3.2 ± 0.2, runner + saline, 4.6 ± 0.2; all in $\Delta F/F_0$, $P < 0.0001$; Fig. 3, D and E). No significant change, however, was found when enumerating the total number of calcium transients ($P > 0.05$; fig. S4, A and B). We then asked whether mTOR activation was also involved in exercise-induced neuronal activity by rapamycin administration (Fig. 3B). The pharmaceutical inhibition of mTOR eliminated exercise-elevated calcium peak amplitudes ($P < 0.05$; Fig. 3, D and E) but did not affect frequencies ($P > 0.05$; fig. S4). Together, both ex vivo and in vivo recordings demonstrate the involvement of exercise-activated mTOR in facilitating synaptic transmissions and neuronal activities.

Exercise training increases axonal myelination by activating mTOR

Axonal myelination is necessary for neural network processing and can be conferred by optogenetic excitation of cortical pyramidal neurons (*40*). As our in vivo calcium imaging has demonstrated potentiated neuronal activities after the exercise training, we further investigated the myelination pattern (Fig. 4, A and B). First, the intensity of myelin basic protein was elevated in medial corpus callosum (CC) regions, where L5PRN send out their projecting fibers. This enhancement in exercised mice also followed mTOR-dependent manners ($P = 0.0003$; Fig. 4, C and D). An EM-based morphometry study was then performed and found exercise-induced thickening of the myelin sheath, which was weakened after rapamycin injection (Fig. 4E). The *g*-ratio, which is calculated as the axonal perimeter

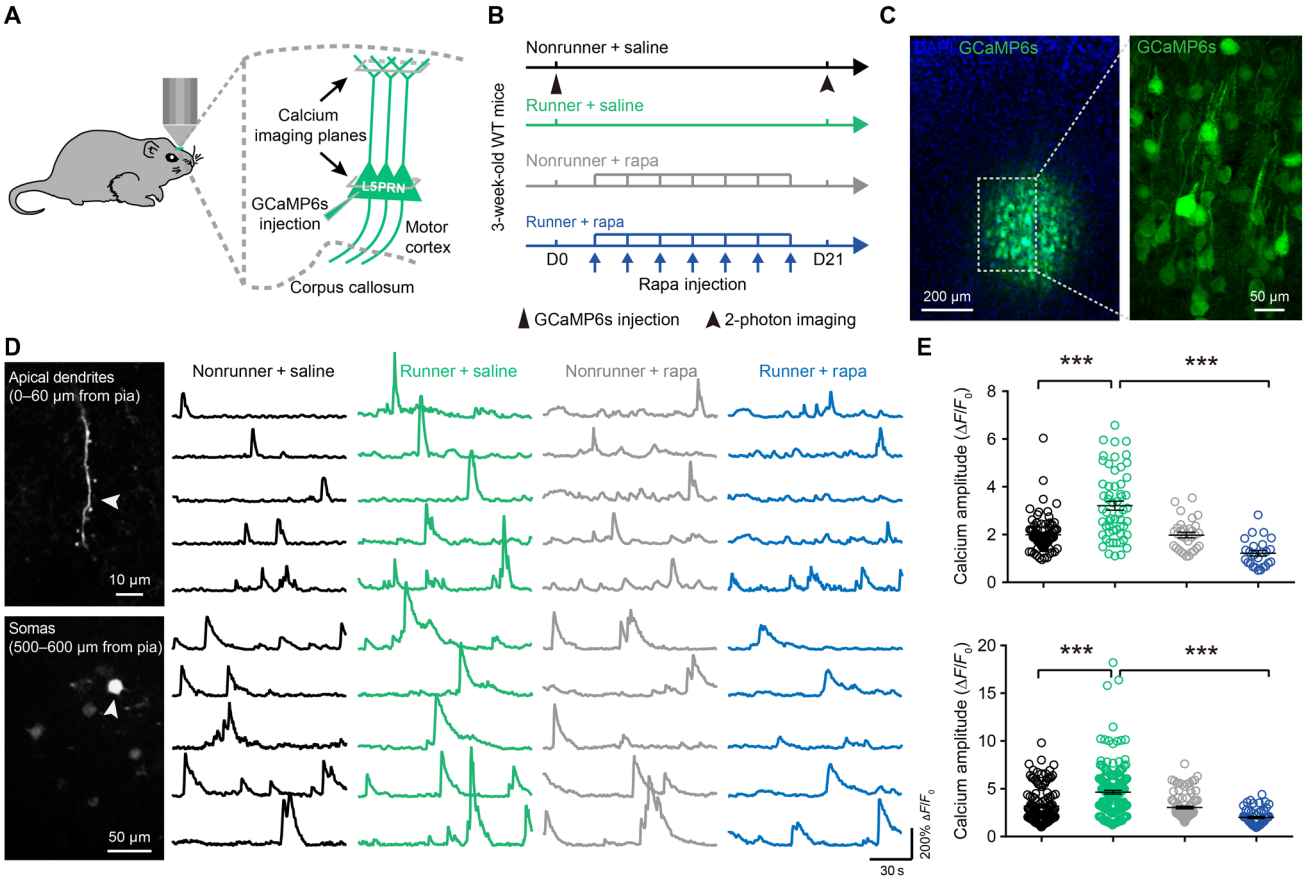

Fig. 3. Exercise training enhances neuronal activity in vivo. (**A**) Illustrations of in vivo calcium recordings for apical dendrites and somas of L5PRN. (**B**) Schematic diagram of experimental protocols. Mice received AAV-GCaMP6s virus injection before 21-day treadmill training. Rapamycin was administrated every 3 days. At the end of exercise training, calcium imaging was performed. (**C**) Coronal section of mouse primary motor cortex showing GCaMP6s-transfected neurons after 3 weeks. (**D**) Representative *z*-stacked imaging planes (left) and calcium fluorescent traces (right) obtained from apical dendrites (top) and somas (bottom) of L5PRN. White arrowheads, active apical dendrite or somas. (**E**) Quantification of calcium peak $\Delta F/F_0$ values in apical dendrites (top) and somas (bottom). Runner mice showed significantly higher peak values (apical dendrite: one-way ANOVA, $F_{3,195} = 16.89$, $P < 0.0001$; Tukey post hoc comparison, $q_{195} = 10.58$, $P < 0.0001$ for nonrunner + saline versus runner + saline and $q_{27} = 12.33$, $P < 0.0001$ for runner + saline versus runner + rapamycin; soma: $F_{3,456} = 14.78$, $P < 0.0001$; $q_{456} = 8.683$ and $P < 0.0001$ for nonrunner + saline versus runner + saline and $q_{456} = 12.03$, $P < 0.0001$ for runner + saline versus runner + rapamycin). ***$P < 0.001$. $n = 6$ animals in each group. Error bars, SEM.

divides the myelin sheath perimeter, also suggested facilitated myelination in the exercised mice (runner + saline, 0.74 ± 0.07; nonrunner + saline, 0.82 ± 0.05; $P < 0.0001$; Fig. 4F). Rapamycin injection abolished this enhancements of myelination (runner + rapamycin, 0.87 ± 0.04; $P < 0.0001$ comparing to runner + saline group; Fig. 4F), supporting the necessary role of mTOR activation.

We then explored the cellular mechanism for exercise-enhanced myelination. Myelin sheath is formed by oligodendrocytes (OLs) that are differentiated from their progenitor cells (OPCs). We injected 5-bromo-2-deoxyuridine (BrdU) during the last 5 days of the 21-day exercise paradigm to label newly formed cells (Fig. 4G). In runner mice, we found more $BrdU^+$ cells within the CC region ($P < 0.0001$; Fig. 4, H and I). Those $BrdU^+$ cells were not microglial or astrocytes (fig. S5), but mostly belonged to OLs lineage in the CC region ($Olig2^+BrdU^+$; $P = 0.0058$; Fig. 4, J and N) or in the motor cortex (fig. S6). Exercised mice had more OPCs ($PDGFR\alpha^+BrdU^+$; $P = 0.0002$; Fig. 4, K and O] and more matured OLs ($CC1^+BrdU^+$; $P = 0.0008$; Fig. 4, L and P). These exercise-enhanced OL-populating events were dependent on mTOR activation (runner + saline versus runner + rapamycin, $P < 0.001$ for $Olig2^+BrdU^+$, $PDGFR\alpha^+BrdU^+$, and $CC1^+BrdU^+$; Fig. 4, N to P). Moreover, fewer newly generated OLs stayed in the proliferating phase in runner mice ($Ki67^+BrdU^+$; $P = 0.031$; Fig. 4, M and Q). Together, the treadmill exercise enhances OPCs proliferation and promotes their differentiation toward mature OLs for enhancing axonal myelination, which is dependent on mTOR activation.

Exercise training persistently promotes dendritic spine formation and enhances motor learning

After demonstrating enhanced neural activity and axonal myelination in exercised mice, we next asked whether the learning function can be improved. A single bout of motor learning task induces the formation of dendritic spines (*19*), which may constitute the structural basis of motor memory (*18*). We thus examined the dendritic spine formation of L5PRN apical tufts using Thy1–yellow fluorescent protein (YFP) transgenic mice during treadmill paradigms (Fig. 5, A to C). The chronic training persistently elevated spine turnover and formation rates (runner versus nonrunner: turnover rates, 15.1 ± 0.5% versus 10.2 ± 0.4% at day 3, 22.1 ± 0.6% versus 14.0 ± 0.7% at day 7, and 30.5 ± 0.9% versus 26.5 ± 0.6% at day 15; $F_{1,36} = 127.1$, $P < 0.0001$; Fig. 5D; formation rates, 10.2 ± 0.4% versus 5.0 ± 0.2%

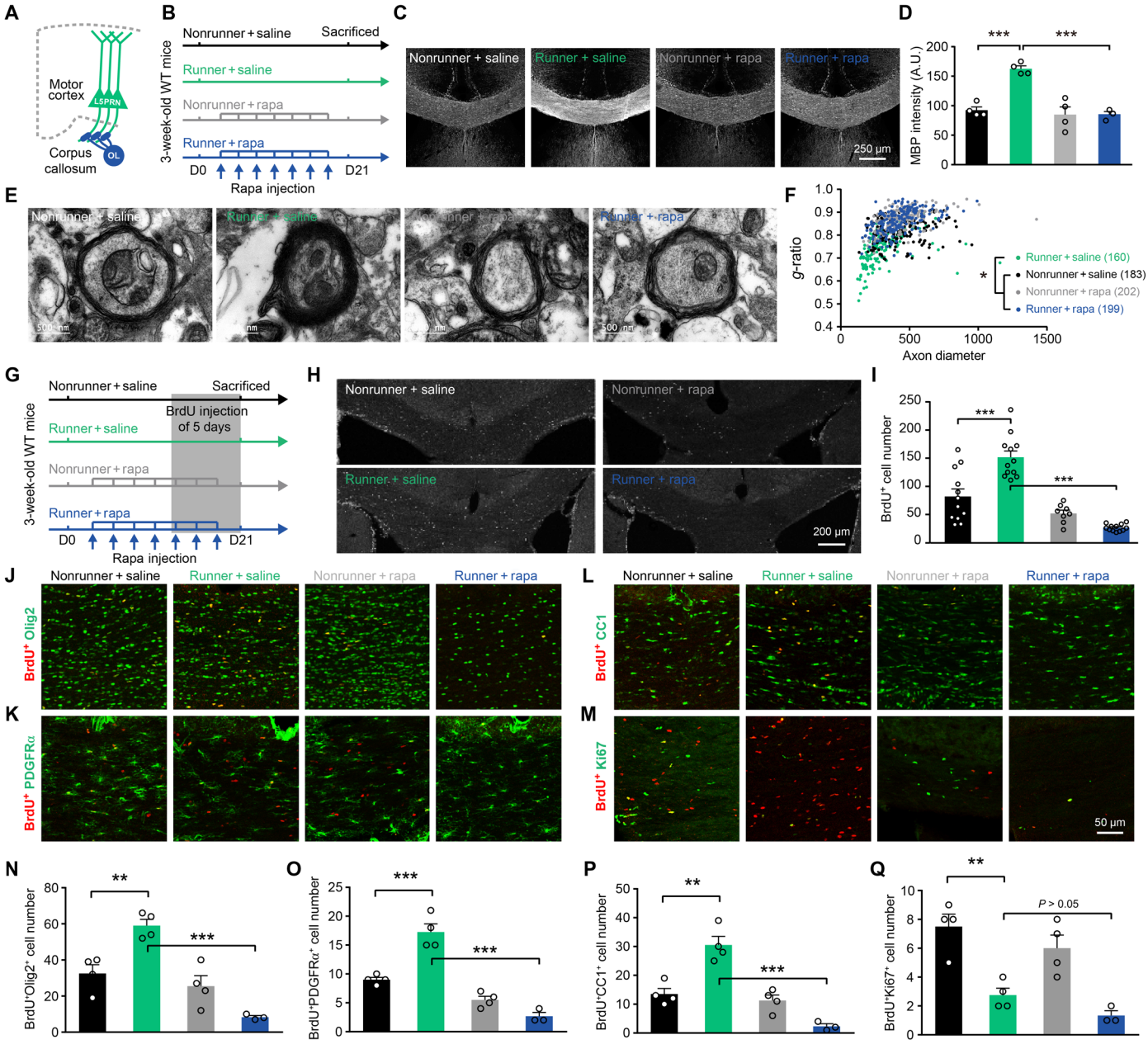

Fig. 4. The activation of mTOR is necessary for exercise-enhanced axonal myelination in the CC region. (**A**) Illustrations of L5PRN axonal myelination, which is formed by mature oligodendrocytes (OLs) in the CC region. (**B**) Schematic diagrams of experimental protocols. Mice received 21-day exercise and rapamycin or saline injection every 3 days. (**C**) Representative images for myelin basic protein (MBP) staining in the medial CC region. Scale bar, 250 μm. (**D**) Quantitative analysis of fluorescent intensities of MBP ($n = 4$ animals in each group) showed elevated myelination level in runner + saline group (one-way ANOVA, $F_{3,11} = 3.353$, $P = 0.0591$; Tukey post hoc test, $q_{11} = 8.721$, $P = 0.0003$) and subsequent decrease after mTOR inhibition ($q_{11} = 8.852$, $P = 0.0003$). A.U., arbitrary units. (**E**) EM images showing myelinated axonal fibers. Scale bars, 500 nm. (**F**) Distribution of *g*-ratios. Kruskal-Wallis test showed significantly lower *g*-ratios in runner + saline mice comparing to nonrunner + saline group ($P < 0.0001$). (**G**) Schematic illustrations for the experimental design of oligodendrogenesis. Daily 5-bromo-2-deoxyuridine (BrdU) injections were given during the last 5 days of exercise training. (**H**) Representative images of BrdU-incorporated ($BrdU^+$) cells in the medial CC region. Scale bar, 200 μm. (**I**) Chronic exercise increased $BrdU^+$ cells ($F_{3,40} = 6.727$, $P < 0.001$; $q_{40} = 7.519$, $P < 0.0001$), and rapamycin injection significantly decreased $BrdU^+$ cells ($q_{40} = 13.51$, $P < 0.0001$). (**J** to **M**) Double immunostaining of $BrdU^+$ cells with OL linage marker Olig2 (J), OL progenitor cells (OPCs) marker PDGFRα (K), mature OL marker CC1 (L), and cell proliferation marker Ki67 (M). Scale bar, 50 μm. (**N** to **P**) Quantification across groups showed that exercise increased the number of $Olig2^+BrdU^+P$ ($F_{3,11} = 20.89$, $P < 0.0001$; $q_{11} = 6.084$, $P = 0.0058$) (N), $BrdU^+PDGFR\alpha^+$-labeled OPCs ($F_{3,11} = 47.05$, $P < 0.0001$; $q_{11} = 9.328$, $P = 0.0002$) (O), and $BrdU^+CC1^+$-labeled, matured OL ($F_{3,11} = 27.16$, $P < 0.0001$; $q_{11} = 7.906$, $P = 0.0008$) (P) after exercise. The OLs proliferation and maturation were reduced by rapamycin treatment (runner + saline versus runner + rapamycin groups: $BrdU^+Olig2^+$, $q_{11} = 10.77$, $P < 0.0001$; $BrdU^+PDGFR\alpha^+$, $q_{11} = 15.27$, $P < 0.0001$; $BrdU^+CC1^+$, $q_{11} = 12.13$, $P < 0.0001$). (**Q**) Exercise also facilitated OL differentiation as suggested by fewer $BrdU^+Ki67^+$ cells ($F_{3,11} = 14.26$, $P = 0.0004$; $q_{11} = 6.655$, $P = 0.0031$), which was not affected by mTOR (runner + saline versus runner + rapamycin groups, $q_{11} = 1.838$, $P = 0.5819$). $^*P < 0.05$, $^{**}P < 0.01$, $^{***}P < 0.001$. $n = 4$ animals in each group. Error bars, SEM.

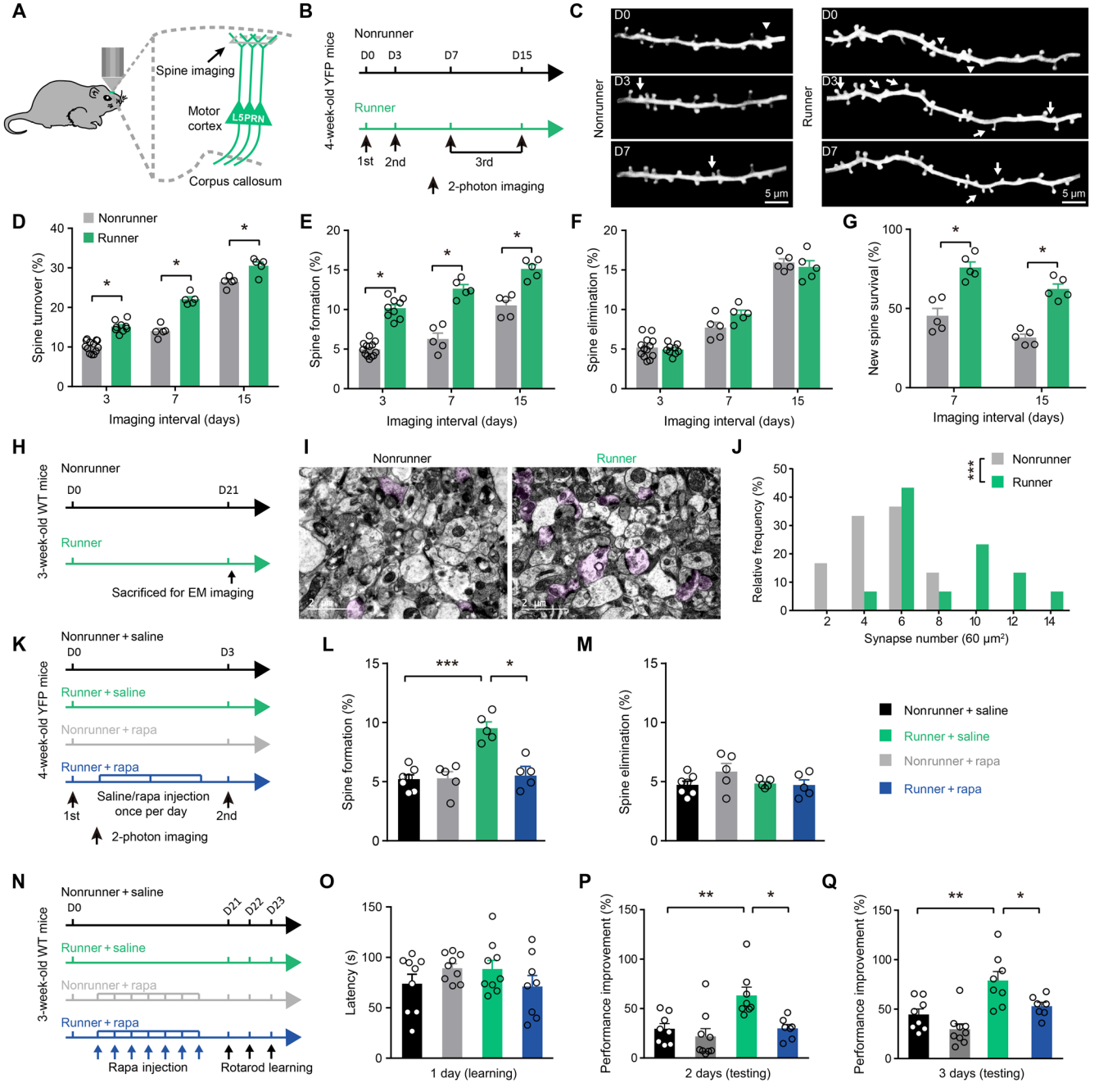

Fig. 5. Treadmill exercise promotes cortical dendritic spine formations and motor learning via mTOR activation. (**A**) Illustration of Thy1-YFP mice and imaging planes. (**B**) Schematic diagram of experimental protocols. Mice received treadmill exercise from days 0 to 15 and were imaged on the same region of primary motor cortex on days 0, 3, and 7 or 15. (**C**) *Z*-axis stacked images showing the same dendritic branches of L5PRNs at day 0 (first imaging), day 3 (second imaging), and day 7 (third imaging) between runner or nonrunner mice. Arrowheads, eliminated spines; arrows, newly formed spines. Scale bars, 5 μm. (**D**) Overall spine turnover rates of runner mice were higher than nonrunner animals [two-way ANOVA$_{(\text{group effect})}$, $F_{1,36} = 127.1$, $P < 0.0001$]. (**E**) Spine formation rates of L5PRN were persistently increased in runner mice compared to nonrunner controls [two-way ANOVA$_{(\text{group effect})}$, $F_{1,36} = 184.4$, $P < 0.0001$]. (**F**) Spine elimination was not affected [two-way ANOVA$_{(\text{group effect})}$, $F_{1,36} = 0.5791$, $P = 0.4516$]. (**G**) Newly formed spines on day 3 had higher survival rates in exercised mice on days 7 or 15 [two-way ANOVA$_{(\text{group effect})}$, $F_{1,24} = 79.33$, $P < 0.0001$]. (**H**) Experimental protocols and (**I**) representative images of EM showing pre- and postsynaptic (in pink color) complexes in the motor cortex. Scale bars, 2 μm. (**J**) Histogram showed more synapses in runner mice (two-sample student *t* test, $t_{58} = 5.791$, $P < 0.001$). (**K**) Schematic illustration studying the effect of mTOR on spinogenesis. Rapamycin was applied daily for 3 days between repeated imaging. (**L**) Rapamycin treatment significantly decreased exercise-induced spine formation (one-way ANOVA, $F_{3,18} = 15.75$, $P < 0.0001$; Tukey's post hoc test, $q_{18} = 6.234$, $P = 0.0018$). (**M**) Elimination of spines was not affected ($F_{3,18} = 1.508$, $P = 0.2465$). (**N**) Experimental designs of accelerating rotarod assay. (**O**) Similar motor performances on day 1 (nonrunner + saline, $n = 8$; runner + saline, $n = 8$; nonrunner + rapamycin, $n = 9$; runner + rapamycin, $n = 8$). (**P** and **Q**) Improvements of motor performances (in percentage) on days 2 and 3. Exercised significantly improved motor learning that was abolished by rapamycin injection (day 2: one-way ANOVA, $F_{3,28} = 7.43$, $P = 0.0008$; Tukey's post hoc test, $q_{28} = 4.70$, $P < 0.05$; day 3: $F_{3,28} = 10.64$, $P < 0.0001$; $q_{28} = 3.88$, $P < 0.05$). *$P < 0.05$, **$P < 0.01$, ***$P < 0.001$. Error bars, SEM.

at day 3, 12.6 ± 0.5% versus 6.3 ± 0.7% at day 7, and 15.1 ± 0.5% versus 10.5 ± 0.6% at day 15; $F_{1,36}$ = 184.1, P < 0.0001; Fig. 5E). The spine elimination rate, however, was not affected ($F_{1,36}$ = 0.5791, P = 0.4516; Fig. 5F). Consistent with our previous findings in barrel cortex (*12*), physical exercise increased the survival rate of day 3 newly formed spines in the motor cortex (runner versus nonrunner, 75.9 ± 3.5% versus 45.0 ± 4.6% at day 7 and 62.4 ± 3.1% versus 31.3 ± 2.1% at day 15; $F_{1,24}$ = 79.33, P < 0.0001; Fig. 5G). By EM examination, we also found elevated synapse densities in the motor cortex from exercised mice (t_{58} = 5.791, P < 0.0001; Fig. 5, I and J). In summary, exercise training facilitates the dendritic spine formation of the motor cortex. The mTOR pathway can regulate spinogenesis both in vitro (*41*) and in vivo (*14*), and we thus examined the role of mTOR in exercise-induced spine formation. After daily rapamycin injection during 3-day treadmill exercise (Fig. 5K), we totally abolished the exercise-enhanced spine formation without sacrificing the basal level of spinogenesis (nonrunner + saline, 5.2 ± 0.4%; nonrunner + rapamycin, 5.3 ± 0.6%; runner, 9.5 ± 0.5%; runner + rapamycin, 6.4 ± 0.6%; $F_{3,18}$ = 15.75, P < 0.0001; Fig. 5L). No effect was observed on spine elimination rates (Fig. 5M). These data collectively suggested that chronic exercise activates mTOR for facilitating new spine formation in the motor cortex.

Motor skill learning can be improved by enhanced spine formation (*42*), cortical network activity (*43*), and axonal myelination (*22*), all of which have been observed in exercised mice. We thus asked whether the exercise training helps to enhance the motor learning function using the accelerating rotarod test (Fig. 5N). Similar performances at the first test session (Fig. 5O) suggested minimal effects from the muscular strength that may also be enhanced by the exercise. With repeated training, exercised mice showed better acquisitions as indicated by higher percentages of performance improvements (runner versus nonrunner, 63.3 ± 8.3% versus 29.5 ± 5.3% at day 2 and 78.8 ± 9.1% versus 44.5 ± 5.6% at day 3; q_{28} = 4.94 and 5.32 for days 2 and 3, respectively, P < 0.01; Fig. 5, P and Q). Rapamycin inhibition assay further demonstrated that the mTOR activation is necessary for this exercised-enhanced motor learning (runner + rapamycin, 30.0 ± 4.0% on day 2 and 52.9 ± 4.0% on day 3; q_{28} = 4.70 and 3.89 comparing between runner + rapamycin and runner + saline groups at days 2 and 3, respectively, P < 0.05; Fig. 5, P and Q). Together, chronic exercise training activates mTOR pathway to induce motor cortex remodeling, including enhanced spinogenesis and synaptic transmissions, potentiated neuronal activities, and increased axonal myelinations, all of which further contribute to better motor learning functions.

DISCUSSION

The current study, to our knowledge, provides the first piece of in vivo evidence showing that the exercise training enhances motor skill learning via mTOR-dependent spinogenesis, neuronal activity, and axonal myelination. Despite dozens of studies reporting the beneficiary effects of exercise on learning and memory functions, little has been known about its molecular basis besides the BDNF model. Our results thus identify one critical intracellular pathway for the exercise mediation of cognitive functions and address the long-standing question for the role of mTOR underlying structural and functional adaptations of neural networks in response to the exercise (*44*). Previous findings supported the improvement of hippocampal neurogenesis and spinogenesis by the voluntary running (*45*) and enhanced spine survival in mouse barrel cortex after the treadmill exercise (*12*). The current data broaden our understandings for central effects of exercise, which leads to the neural remodeling covering spines or synapses, neuronal somas, and axons. Those structural and functional enhancements help to explain the improved learning after the exercise training.

We obtained higher mEPSC amplitudes but unchanged frequencies of L5PRN in the motor cortex in exercised mice, indicating enhanced postsynaptic transmissions rather than presynaptic vesicle release. These data are consistent with stronger calcium transients of L5PRN in awake mice by in vivo recordings. These enhanced neural transmissions have a structural basis, including the elevated synthesis of postsynaptic protein PSD95. Although presynaptic protein SNAP25 was also modestly elevated by exercise training, no change was found in synaptophysin (Fig. 1D), which is critical for presynaptic vesicle release (*46*). The enhanced synaptic transmission was further substantiated by the EM study, which showed elongation and thickening of PSD complexes (Fig. 1, E to G). These exercise-induced structural alternations help to facilitate the excitatory postsynaptic transmission via mTOR activation. It also agrees with previous knowledge showing the facilitation of synaptic protein synthesis by mTOR-S6 activation (*38*), resulting in potentiated synaptic transmissions (*39*). As both enhanced synaptic transmissions and neuronal activities benefit the acquirement of complex motor skills (*43*, *47*), our studies strongly suggest the facilitation of motor memory acquisitions by exercise training via mTOR-mediated neural activities.

Besides enhanced synaptic transmissions and neuronal activities, long-term treadmill exercise also facilitates the axonal myelination within CC regions, where the majority of L5PRN forms efferent fibers. Although enhanced myelination may limit the axonal growth during the critical developmental period to impair the neural plasticity (*48*), enhanced adult myelination has been reported to improve motor learning functions (*22*). Recent findings suggest that myelination is one highly dynamic process that can be potentiated by neuron activities in adult mice (*49*). Therefore, the exercise-induced myelination in this study is probably caused by mTOR-enhanced neuron activities. An alternative explanation also exists, as mTOR activation facilitates OPCs proliferation and differentiation to enhance axonal myelination (*31*, *32*, *50*). Our cell linage studies partially support this model, as endurance training facilitates de novo OPCs proliferation and differentiation that are dependent on mTOR activation. One question remains about the mechanism governing exercise-induced OPCs proliferation, which can be caused by the enhanced neuron activity as in previous findings (*40*), or the cell-autonomous regulation by mTOR in OPCs. The cell-specific deprivation of mTOR activity can address this issue in future. It is further noticed that the overactivation of mTOR in *Tsc1* gene knockout mice leads to hypomyelination (*51*). Although seemingly contradictory to our observations showing exercise-activated mTOR activation for enhanced myelination, these data highlight the pivotal role of maintaining mTOR activity within normal physiological ranges for axonal myelination.

Runner + rapamycin mice presented even lower neuronal activities (Figs. 2I and 3E) and worse oligodendrogenesis (Fig. 4, I to P) compared to nonrunner + rapamycin animals. This difference suggests that exercise may not directly activate mTOR pathway in a straightforward manner. Accumulating studies have shown that mTOR works as one "energy sensor" and can be activated upon higher

metabolic rates of cells (*52*). We thus examined the level of phosphorylated adenosine 5′-monophosphate–activated protein kinase (p-AMPK), which is one sensitive marker for cellular energy requirements (*53*). Only runner + rapamycin mice presented higher p-AMPK levels compared the other three groups (fig. S7, A and B). This evidence supports that exercise elevates the energy requirement, which is subsequently satisfied by mTOR activation [fig. S7C, scenario (i)], and further rapamycin inhibition of mTOR leads to insufficient energy supply in exercised brain tissues, causing impaired cell activities [fig. S7C, scenario (ii)]. In addition, AMPK phosphorylation can further suppress the mTOR pathway (*53*), thus exerting synergistic effects with rapamycin to further down-regulate cell activities. Last, nonrunner + rapamycin mice displayed normal cell activity or oligodendrogenesis because mTOR activation is not necessary under low energy requirement [fig. S7C, scenario (iii)]. This feedback model of exercise activation of mTOR supports its roles under metabolic stress of brain tissues, similar to those in peripheral organs (*54*).

Motor learning in adult brains is associated with cortical spine plasticity (*19*), which can be impaired by glucocorticoid or physically restrained stress causing memory loss (*55*, *56*), and can be improved by environment enrichment (*56*) or physical exercises (*12*). In motor cortex, a single bout of motor learning rapidly stimulates spinogenesis (*57*), which lays the structural basis for motor memory consolidations (*18*). Our data suggest that dendritic spines can be generated and maintained during the exercise training. This exercise-induced spine formation is different from previously reported phenotypes after short-term motor learning, as being interpreted from two aspects: First, rotarod learning can induce branch-specific spine formations (*57*), while our exercised mice did not present branch-dependent patterns of spinogenesis. Second, the majority of motor learning–induced newly formed spines disappeared within days (*58*), while exercise-associated spinogenesis can be sustained for up to 14 days. We thus argue that the physical exercise promotes spinogenesis of motor cortex in a more persistent and broadened manner. Mechanistic studies showed that mTOR activation is necessary for exercise-mediated spine formation but not for basal levels of spine formation or maintenance (Fig. 5, M and N). Our data thus establish the necessary role of mTOR in exercise-promoted spinogenesis, which provides the structural basis for improved motor learning. Nevertheless, the modulation of exercise training on different cortical neuron subtypes other than the L5PRN is not investigated here and may provide more insights for exercise-induced neural remodeling.

In summary, exercise activates mTOR to improve motor skill learning, which can be attributed to the enhancement of spinogenesis, synaptic transmissions, neuron activities, and axonal myelinations. The activation of mTOR is necessary for cortical neural remodeling and improves motor learning under exercise paradigms. One may expect that mTOR activation directs exercise-induced enhancements of other learning and memory paradigms. Our results collectively establish the central role of mTOR pathway for neural network adaptations to exercises and provide more evidence for clinical intervention of psychiatric diseases and cognitive deficits using exercise training.

MATERIALS AND METHODS

Experimental design

Male C57BL/6J mice (4 weeks old) were purchased from Guangdong Medical Laboratory Animal Center and were used for Western blotting, in vivo calcium recording, BrdU incorporation assay, and behavioral assays. Male Thy1-YFP transgenic mice (4 weeks old) were obtained from the Jackson Laboratory (Bar Harbor, ME) and were bred in house. Thy1-YFP mice were used for in vivo dendritic spine imaging and patch-clamp recording. The exact *n* number for each experiment was specified in relevant result or figure legend sections. All animals were group-housed under normal light-dark cycle with food and water ad libitum. All animal experimental protocols were preapproved by the Ethics Committee of Experimental Animals of Jinan University in accordance with Institutional Animal Care and Use Committee guidelines for animal research.

The treadmill exercise was performed as previously described (*12*). One six-channel treadmill apparatus (Model JD-PT, Jide Instruments, Shanghai, China) was adopted (12 m/min, 1 hour daily, for 3 weeks unless otherwise specified). Control (nonrunner) mice were put onto the fixed treadmill device for 1 hour within the same environment. After 21-day treadmill exercise training, animals were sacrificed for further assays. For in vivo spine imaging, Thy1-YFP animals received the first imaging before exercise initiation and were reimaged on exercise day 3, 7, or 14. The rapamycin administration (3 mg/kg body weight) was performed every 3 days during the exercise training, or on each day within 3-day treadmill training for spine imaging assays.

Western blotting

Tissue lysates were extracted from the mouse primary motor cortex in radioimmunoprecipitation assay buffer containing protease and phosphatase inhibitors. After quantification using bicinchoninic acid kit (Beyotime, Shanghai, China), 10 μg of protein samples were separated by SDS–polyacrylamide gel electrophoresis under 90 mA for 90 min and were transferred to the polyvinylidene fluoride membrane at 200 V for 30 min. After washing in phosphate-buffered saline (PBS) with Tween 20 and blocking in 5% bovine serum albumin (BSA), the membrane was incubated with the primary antibody (table S1) at 4°C overnight. The membrane was washed and incubated in secondary antibody (table S1) for 2 hours. Protein bands were visualized using an imaging system (Bio-Rad, Hercules, USA). Integrated gray values of each band were measured using ImageJ (National Institutes of Health, Bethesda, USA).

Immunofluorescence staining

Mice were euthanized by isoflurane and were perfused with paraformaldehyde. Whole brain tissues were dehydrated with 30% sucrose overnight and were sectioned into 40-μm coronal slices using a sliding microtome (Leica, Germany). After PBS washing and BSA blocking, the brain slices were incubated with primary antibody at 4°C for 48 hours, followed by secondary antibody (table S1). Images were captured with a confocal microscope (ZEISS, Germany), and the fluorescent intensity was analyzed using ImageJ.

Virus injection and in vivo two-photon calcium imaging

Mice were anesthetized using 1.25% Avertin. After local sterilization and incision of head skins, the primary motor cortex (1.0 mm posterior and 1.5 mm lateral from Bregma) was localized under a stereotaxic instrument (RWD Life Science Inc., China). After drilling a hole by the high-speed microdrill, 0.1 μl of AAV serotype 2/9 carrying genetically encoded calcium indicator GCaMP6s under hSyn promoter (viral titer, $>1 \times 10^{13}$ genome copies/ml; Taitool Bioscience, China) was slowly injected into layer V (500 to 700 μm

from the pia) using a glass micropipette connected to an ultramicro injection pump (Nanoliter 2010, World Precision Instruments, Sarasota, USA). The micropipette was retained for 10 min before retraction. The head skin was closed for postsurgery monitor. The calcium imaging was performed 21 days later.

In vivo calcium recording was performed as previously described (*59*). Briefly, the head skin and skull covering motor cortex were removed to create an imaging window (2 mm by 2 mm), which was covered by a glass coverslip. The calcium activities of apical dendrites (0 to 60 μm from the pia) and layer V somas (500 to 600 μm in depth) were recorded at 2 Hz with a water-immersed objective (20×, 1.1 numerical aperture; ZEISS) during a 2.5-min period under an LSM780 two-photon microscope (ZEISS, Germany). During imaging, the laser was tuned to the 920 nm, and the laser power was restricted below 25 mW.

Acquired time series images were corrected by TurboReg module of ImageJ. The fluorescent value F was quantified by average pixels extracted from designed region of interest covering identifiable soma or apical dendrite with >30 μm in length. The $\Delta F/F_0$ was calculated as $(F - F_0)/F_0$, where the F_0 was averaged F values during the first 10% recording period as the basal level. A calcium transient was defined when the $\Delta F/F_0$ is higher than threefold SDs.

Dendritic spine imaging

In vivo imaging of dendritic spines was performed by creating a thin-skull imaging window as previously described (*60*). Briefly, male Thy1-YFP mice were anesthetized, and the skull was exposed by the incision of head skins. The primary motor cortex was identified as abovementioned, and a circular imaging window was created by a high-speed microdrill. Images of apical dendritic spines were captured at 920-nm laser excitation. Both low-magnification z-stack image and vascular distribution map were recorded for reimaging. About seven high-magnification z-stack images (4× digital zoom, 0.75-μm interval, 1024 × 1024 pixels) were obtained for dendritic spines quantification. After imaging, mice were returned to their own homecage for recovery until reimaging.

The analysis of dendritic spine followed previous publication (*42*). Briefly speaking, acquired stacking images were projected to a single plane with one or more dendrite(s) with signal-to-noise ratio of >3. The same dendritic segment at different time points were compared for spine formation and elimination rates, which are based on the total spine numbers at the first imaging. All geometric measurements and spine enumerations were performed using ImageJ.

Whole-cell patch-clamp recording

Male Thy1-YFP mice were deeply anesthetized with isoflurane. Brain tissues were extracted and dissected into 250-μm coronal slices on a Vibratome (Leica, Germany). Cortical slices were incubated in oxygenated artificial cerebrospinal fluid (aCSF; consisting of 119 mM NaCl, 2.5 mM KCl, 1 mM NaH_2PO_4, 11 mM glucose, 26.2 mM $NaHCO_3$, 2.5 mM $CaCl_2$, and 1.3 mM $MgCl_2$) for 1 hour recovery and were transferred to the recording chamber with continuous perfusion of oxygenated aCSF containing 1 μM tetrodotoxin.

Whole-cell recording was performed on cortical L5PRN as indicated by YFP signals using an epifluorescence microscope (Olympus, Japan). A glass pipette (3- to 5-megohm resistance) was filled with internal solutions [135 mM $CsMeSO_3$, 8 mM NaCl, 10 mM Na_2-phosphocreatine, 0.25 mM EGTA, 2.17 mM Mg–adenosine 5′-triphosphate, 0.34 mM Na_3–guanosine 5′-triphosphate, and 10 mM Hepes (pH 7.4) with CsOH]. Neurons were clamped at −70 and 0 mV for miniature excitatory mEPSCs recording. Traces were collected by a MultiClamp 700B amplifier (Molecular Devices, USA), filtered at 4 kHz, and digitized at 10 kHz (Digidata 1550A, Molecular Devices, USA). Events were analyzed by Clampfit 10.0 (Molecular Devices, USA).

Electron microscopy

EM was performed as previously described (*61*). Briefly, mouse brain tissues were blocked in the fixative reagent (G1102, Servicebio) at 4°C for 2 hours and were postfixed with 1% osmium tetroxide for 2 hours. Tissues were dehydrated in graded ethanol solutions (50 to 100% and two times of acetone, 15 min each) and were embedded in EMbed 812 (90529-77-4, Structure Probe Inc., West Chester, USA) at 60°C for 48 hours. Brain tissues were prepared in ultrathin slices (60 to 80 nm) with an ultramicrotome (Leica EM UC7, Leica). Slices were stained with uranyl acetate in pure ethanol for 15 min, in lead citrate for 15 min and were air-dried. Images were captured with a transmission electron microscope (Hitachi, Japan). Both synapse density and axonal myelination were counted under the 13,500× magnification, postsynaptic (PSD) length and thickness were calculated under 46,000× magnification by ImageJ.

Motor learning behavior

The motor learning ability was assessed by an accelerating rotarod (Ugo Basile, Comerio, Italy), which started at 5 rpm and sped up to 80 rpm within 5 min. Each mouse received three training sessions at 9:00 a.m., with each session on one of three consecutive days.

Statistical analysis

All data were presented as means ± SEM. Two-sample student's t test, one-way analysis of variance (ANOVA), and Tukey post hoc test were used to compare differences among two or multiple groups, respectively. For two independent variables, two-way ANOVA and Bonferroni post hoc comparison were adopted. For comparison of g-ratios, Kruskal-Wallis test was adopted because of non-Gaussian distribution of sample data. A significant level was defined when $P < 0.05$. All statistical analysis was performed by GraphPad Prism 7.0 (La Jolla, CA, USA).

SUPPLEMENTARY MATERIALS

Supplementary material for this article is available at http://advances.sciencemag.org/cgi/content/full/5/7/eaaw1888/DC1

Fig. S1. Exercise-activated ribosomal protein S6 in motor cortex.
Fig. S2. Exercise-induced neuron activity of cortical pyramidal neurons.
Fig. S3. Calcium spike dynamics of apical tuft and soma of L5PRN.
Fig. S4. Calcium transients of L5PRN.
Fig. S5. Subtyping of $BrdU^+$ cells in the CC region.
Fig. S6. Immunofluorescence labeling of BrdU and Olig2 in mouse motor cortex after exercise.
Fig. S7. Energy requirement of cells under exercise.
Table S1. Primary and secondary antibody used in Western blotting and immunofluorescence staining.

REFERENCES AND NOTES

1. C. H. Hillman, K. I. Erickson, A. F. Kramer, Be smart, exercise your heart: Exercise effects on brain and cognition. *Nat. Rev. Neurosci.* **9**, 58–65 (2008).
2. C. Handschin, B. M. Spiegelman, The role of exercise and PGC1α in inflammation and chronic disease. *Nature* **454**, 463–469 (2008).
3. W. Fan, R. M. Evans, Exercise mimetics: Impact on health and performance. *Cell Metab.* **25**, 242–247 (2017).
4. G. M. Petzinger, B. E. Fisher, S. McEwen, J. A. Beeler, J. P. Walsh, M. W. Jakowec, Exercise-enhanced neuroplasticity targeting motor and cognitive circuitry in Parkinson's disease. *Lancet Neurol.* **12**, 716–726 (2013).

5. M. Roig, K. Skriver, J. Lundbye-Jensen, B. Kiens, J. B. Nielsen, A single bout of exercise improves motor memory. *PLOS ONE* **7**, e44594 (2012).
6. M. A. Statton, M. Encarnacion, P. Celnik, A. J. Bastian, A single bout of moderate aerobic exercise improves motor skill acquisition. *PLOS ONE* **10**, e0141393 (2015).
7. C. S. Mang, N. J. Snow, K. P. Wadden, K. L. Campbell, L. A. Boyd, High-intensity aerobic exercise enhances motor memory retrieval. *Med. Sci. Sports Exerc.* **48**, 2477–2486 (2016).
8. G. Wagner, M. Herbsleb, F. de la Cruz, A. Schumann, S. Köhler, C. Puta, H. W. Gabriel, J. R. Reichenbach, K.-J. Bär, Changes in fMRI activation in anterior hippocampus and motor cortex during memory retrieval after an intense exercise intervention. *Biol. Psychol.* **124**, 65–78 (2017).
9. K. Skriver, M. Roig, J. Lundbye-Jensen, J. Pingel, J. W. Helge, B. Kiens, J. B. Nielsen, Acute exercise improves motor memory: Exploring potential biomarkers. *Neurobiol. Learn. Mem.* **116**, 46–58 (2014).
10. K. I. Erickson, M. W. Voss, R. S. Prakash, C. Basak, A. Szabo, L. Chaddock, J. S. Kim, S. Heo, H. Alves, S. M. White, T. R. Wojcicki, E. Mailey, V. J. Vieira, S. A. Martin, B. D. Pence, J. A. Woods, E. McAuley, A. F. Kramer, Exercise training increases size of hippocampus and improves memory. *Proc. Natl. Acad. Sci. U.S.A.* **108**, 3017–3022 (2011).
11. C. D. Wrann, J. P. White, J. Salogiannnis, D. Laznik-Bogoslavski, J. Wu, D. Ma, J. D. Lin, M. E. Greenberg, B. M. Spiegelman, Exercise induces hippocampal BDNF through a PGC-1α/FNDC5 pathway. *Cell Metab.* **18**, 649–659 (2013).
12. K. Chen, L. Zhang, M. Tan, C. S. W. Lai, A. Li, C. Ren, K.-F. So, Treadmill exercise suppressed stress-induced dendritic spine elimination in mouse barrel cortex and improved working memory via BDNF/TrkB pathway. *Transl. Psychiatry* **7**, e1069 (2017).
13. A. E. Autry, M. Adachi, E. Nosyreva, E. S. Na, M. F. Los, P.-f. Cheng, E. T. Kavalali, L. M. Monteggia, NMDA receptor blockade at rest triggers rapid behavioural antidepressant responses. *Nature* **475**, 91–95 (2011).
14. N. Li, B. Lee, R.-J. Liu, M. Banasr, J. M. Dwyer, M. Iwata, X.-Y. Li, G. Aghajanian, R. S. Duman, mTOR-dependent synapse formation underlies the rapid antidepressant effects of NMDA antagonists. *Science* **329**, 959–964 (2010).
15. F. Sun, K. K. Park, S. Belin, D. Wang, T. Lu, G. Chen, K. Zhang, C. Yeung, G. Feng, B. A. Yankner, Z. He, Sustained axon regeneration induced by co-deletion of PTEN and SOCS3. *Nature* **480**, 372–375 (2011).
16. M. Costa-Mattioli, L. M. Monteggia, mTOR complexes in neurodevelopmental and neuropsychiatric disorders. *Nat. Neurosci.* **16**, 1537–1543 (2013).
17. B. K. Kennedy, D. W. Lamming, The mechanistic target of rapamycin: The grand conducTOR of metabolism and aging. *Cell Metab.* **23**, 990–1003 (2016).
18. A. Hayashi-Takagi, S. Yagishita, M. Nakamura, F. Shirai, Y. I. Wu, A. L. Loshbaugh, B. Kuhlman, K. M. Hahn, H. Kasai, Labelling and optical erasure of synaptic memory traces in the motor cortex. *Nature* **525**, 333–338 (2015).
19. G. Yang, F. Pan, W.-B. Gan, Stably maintained dendritic spines are associated with lifelong memories. *Nature* **462**, 920–924 (2009).
20. P. Martínez-Vazquez, A. Gail, Directed interaction between monkey premotor and posterior parietal cortex during motor-goal retrieval from working memory. *Cereb. Cortex* **28**, 1866–1881 (2018).
21. P. Rajasethupathy, S. Sankaran, J. H. Marshel, C. K. Kim, E. Ferenczi, S. Y. Lee, A. Berndt, C. Ramakrishnan, A. Jaffe, M. Lo, C. Liston, K. Deisseroth, Projections from neocortex mediate top-down control of memory retrieval. *Nature* **526**, 653–659 (2015).
22. I. A. McKenzie, D. Ohayon, H. Li, J. P. de Faria, B. Emery, K. Tohyama, W. D. Richardson, Motor skill learning requires active central myelination. *Science* **346**, 318–322 (2014).
23. K. Watson, K. Baar, mTOR and the health benefits of exercise. *Semin. Cell Dev. Biol.* **36**, 130–139 (2014).
24. C. A. Goodman, The role of mTORC1 in regulating protein synthesis and skeletal muscle mass in response to various mechanical stimuli. *Rev. Physiol. Biochem. Pharmacol.* **166**, 43–95 (2014).
25. M. J. Drummond, H. C. Dreyer, C. S. Fry, E. L. Glynn, B. B. Rasmussen, Nutritional and contractile regulation of human skeletal muscle protein synthesis and mTORC1 signaling. *J. Appl. Physiol.* **106**, 1374–1384 (2009).
26. W. Apro, L. Wang, M. Pontén, E. Blomstrand, K. Sahlin, Resistance exercise induced mTORC1 signaling is not impaired by subsequent endurance exercise in human skeletal muscle. *Am. J. Physiol. Endocrinol. Metab.* **305**, E22–E32 (2013).
27. J. M. Dwyer, J. G. Maldonado-Avilés, A. E. Lepack, R. J. DiLeone, R. S. Duman, Ribosomal protein S6 kinase 1 signaling in prefrontal cortex controls depressive behavior. *Proc. Natl. Acad. Sci. U.S.A.* **112**, 6188–6193 (2015).
28. G. Tang, K. Gudsnuk, S.-H. Kuo, M. L. Cotrina, G. Rosoklija, A. Sosunov, M. S. Sonders, E. Kanter, C. Castagna, A. Yamamoto, Z. Yue, O. Arancio, B. S. Peterson, F. Champagne, A. J. Dwork, J. Goldman, D. Sulzer, Loss of mTOR-dependent macroautophagy causes autistic-like synaptic pruning deficits. *Neuron* **83**, 1131–1143 (2014).
29. S. A. Buffington, W. Huang, M. Costa-Mattioli, Translational control in synaptic plasticity and cognitive dysfunction. *Annu. Rev. Neurosci.* **37**, 17–38 (2014).
30. K. Takeuchi, M. J. Gertner, J. Zhou, L. F. Parada, M. V. Bennett, R. S. Zukin, Dysregulation of synaptic plasticity precedes appearance of morphological defects in a Pten conditional knockout mouse model of autism. *Proc. Natl. Acad. Sci. U.S.A.* **110**, 4738–4743 (2013).
31. S. E. Wahl, L. E. McLane, K. K. Bercury, W. B. Macklin, T. L. Wood, Mammalian target of rapamycin promotes oligodendrocyte differentiation, initiation and extent of CNS myelination. *J. Neurosci.* **34**, 4453–4465 (2014).
32. J. Dai, K. K. Bercury, W. B. Macklin, Interaction of mTOR and Erk1/2 signaling to regulate oligodendrocyte differentiation. *Glia* **62**, 2096–2109 (2014).
33. X. Chen, S. Wang, Y. Zhou, Y. Han, S. Li, Q. Xu, L. Xu, Z. Zhu, Y. Deng, L. Yu, L. Song, A. P. Chen, J. Song, E. Takahashi, G. He, L. He, W. Li, C. D. Chen, *Phf8* histone demethylase deficiency causes cognitive impairments through the mTOR pathway. *Nat. Commun.* **9**, 114 (2018).
34. D. Ehninger, S. Han, C. Shilyansky, Y. Zhou, W. Li, D. J. Kwiatkowski, V. Ramesh, A. J. Silva, Reversal of learning deficits in a $Tsc2^{+/-}$ mouse model of tuberous sclerosis. *Nat. Med.* **14**, 843–848 (2008).
35. A. Sato, S. Kasai, T. Kobayashi, Y. Takamatsu, O. Hino, K. Ikeda, M. Mizuguchi, Rapamycin reverses impaired social interaction in mouse models of tuberous sclerosis complex. *Nat. Commun.* **3**, 1292 (2012).
36. S. Peter, M. M. ten Brinke, J. Stedehouder, C. M. Reinelt, B. Wu, H. Zhou, K. Zhou, H.-J. Boele, S. A. Kushner, M. G. Lee, M. J. Schmeisser, T. M. Boeckers, M. Schonewille, F. E. Hoebeek, C. I. De Zeeuw, Dysfunctional cerebellar Purkinje cells contribute to autism-like behaviour in *Shank2*-deficient mice. *Nat. Commun.* **7**, 12627 (2016).
37. J. A. Kleim, S. Chan, E. Pringle, K. Schallert, V. Procaccio, R. Jimenez, S. C. Cramer, *BDNF* val66met polymorphism is associated with modified experience-dependent plasticity in human motor cortex. *Nat. Neurosci.* **9**, 735–737 (2006).
38. A. Bhattacharya, H. Kaphzan, A. C. Alvarez-Dieppa, J. P. Murphy, P. Pierre, E. Klann, Genetic removal of p70 S6 kinase 1 corrects molecular, synaptic, and behavioral phenotypes in fragile X syndrome mice. *Neuron* **76**, 325–337 (2012).
39. A. R. Luft, M. M. Buitrago, T. Ringer, J. Dichgans, J. B. Schulz, Motor skill learning depends on protein synthesis in motor cortex after training. *J. Neurosci.* **24**, 6515–6520 (2004).
40. E. M. Gibson, D. Purger, C. W. Mount, A. K. Goldstein, G. L. Lin, L. S. Wood, I. Inema, S. E. Miller, G. Bieri, J. B. Zuchero, B. A. Barres, P. J. Woo, H. Vogel, M. Monje, Neuronal activity promotes oligodendrogenesis and adaptive myelination in the mammalian brain. *Science* **344**, 1252304 (2014).
41. Y.-T. Shih, Y.-P. Hsueh, VCP and ATL1 regulate endoplasmic reticulum and protein synthesis for dendritic spine formation. *Nat. Commun.* **7**, 11020 (2016).
42. W. Li, L. Ma, G. Yang, W.-B. Gan, REM sleep selectively prunes and maintains new synapses in development and learning. *Nat. Neurosci.* **20**, 427–437 (2017).
43. A. J. Peters, S. X. Chen, T. Komiyama, Emergence of reproducible spatiotemporal activity during motor learning. *Nature* **510**, 263–267 (2014).
44. M. P. Mattson, K. Moehl, N. Ghena, M. Schmaedick, A. Cheng, Intermittent metabolic switching, neuroplasticity and brain health. *Nat. Rev. Neurosci.* **19**, 63–80 (2018).
45. S. Y. Yau, A. Li, R. L. C. Hoo, Y. P. Ching, B. R. Christie, T. M. C. Lee, A. Xu, K.-F. So, Physical exercise-induced hippocampal neurogenesis and antidepressant effects are mediated by the adipocyte hormone adiponectin. *Proc. Natl. Acad. Sci. U.S.A.* **111**, 15810–15815 (2014).
46. A. Bacci, S. Coco, E. Pravettoni, U. Schenk, S. Armano, C. Frassoni, C. Verderio, P. De Camilli, M. Matteoli, Chronic blockade of glutamate receptors enhances presynaptic release and downregulates the interaction between synaptophysin-synaptobrevin–vesicle-associated membrane protein 2. *J. Neurosci.* **21**, 6588–6596 (2001).
47. J. M. Conner, A. Culberson, C. Packowski, A. A. Chiba, M. H. Tuszynski, Lesions of the basal forebrain cholinergic system impair task acquisition and abolish cortical plasticity associated with motor skill learning. *Neuron* **38**, 819–829 (2003).
48. A. W. McGee, Y. Yang, Q. S. Fischer, N. W. Daw, S. M. Strittmatter, Experience-driven plasticity of visual cortex limited by myelin and Nogo receptor. *Science* **309**, 2222–2226 (2005).
49. R. D. Fields, A new mechanism of nervous system plasticity: Activity-dependent myelination. *Nat. Rev. Neurosci.* **16**, 756–767 (2015).
50. S. Goebbels, G. L. Wieser, A. Pieper, S. Spitzer, B. Weege, K. Yan, J. M. Edgar, O. Yagensky, S. P. Wichert, A. Agarwal, K. Karram, N. Renier, M. Tessier-Lavigne, M. J. Rossner, R. T. Káradóttir, K.-A. Nave, A neuronal $PI(3,4,5)P_3$-dependent program of oligodendrocyte precursor recruitment and myelination. 20, 10–15 (2017).
51. E. Ercan, J. M. Han, A. Di Nardo, K. Winden, M.-J. Han, L. Hoyo, A. Saffari, A. Leask, D. H. Geschwind, M. Sahin, Neuronal CTGF/CCN2 negatively regulates myelination in a mouse model of tuberous sclerosis complex. *J. Exp. Med.* **214**, 681–697 (2017).
52. J. Kim, K.-L. Guan, mTOR as a central hub of nutrient signalling and cell growth. *Nat. Cell Biol.* **21**, 63–71 (2019).
53. D. G. Hardie, F. A. Ross, S. A. Hawley, AMPK: A nutrient and energy sensor that maintains energy homeostasis. *Nat. Rev. Mol. Cell Biol.* **13**, 251–262 (2012).
54. Y. Zhao, X. Hu, Y. Liu, S. Dong, Z. Wen, W. He, S. Zhang, Q. Huang, M. Shi, ROS signaling under metabolic stress: Cross-talk between AMPK and AKT pathway. *Mol. Cancer* **16**, 79 (2017).
55. C. Liston, W.-B. Gan, Glucocorticoids are critical regulators of dendritic spine development and plasticity in vivo. *Proc. Natl. Acad. Sci. U.S.A.* **108**, 16074–16079 (2011).

56. C.-C. Chen, J. Lu, R. Yang, J. B. Ding, Y. Zuo, Selective activation of parvalbumin interneurons prevents stress-induced synapse loss and perceptual defects. *Mol. Psychiatry* **23**, 1614–1625 (2017).
57. G. Yang, C. S. W. Lai, J. Cichon, L. Ma, W. Li, W.-B. Gan, Sleep promotes branch-specific formation of dendritic spines after learning. *Science* **344**, 1173–1178 (2014).
58. C. Liston, J. M. Cichon, F. Jeanneteau, Z. Jia, M. V. Chao, W.-B. Gan, Circadian glucocorticoid oscillations promote learning-dependent synapse formation and maintenance. *Nat. Neurosci.* **16**, 698–705 (2013).
59. A. Holtmaat, T. Bonhoeffer, D. K. Chow, J. Chuckowree, V. De Paola, S. B. Hofer, M. Hübener, T. Keck, G. Knott, W.-C. Lee, R. Mostany, T. D. Mrsic-Flogel, E. Nedivi, C. Portera-Cailliau, K. Svoboda, J. T. Trachtenberg, L. Wilbrecht, Long-term, high-resolution imaging in the mouse neocortex through a chronic cranial window. *Nat. Protoc.* **4**, 1128–1144 (2009).
60. C. S. W. Lai, T. F. Franke, W.-B. Gan, Opposite effects of fear conditioning and extinction on dendritic spine remodelling. *Nature* **483**, 87–91 (2012).
61. J. Feng, Y. Xu, M. Wang, Y. Ruan, K.-F. So, F. Tissir, A. Goffinet, L. Zhou, A role for atypical cadherin *Celsr3* in hippocampal maturation and connectivity. *J. Neurosci.* **32**, 13729–13743 (2012).

Acknowledgments: We thank W. Gan (New York University) for suggestion and help in this study and in revising the manuscript; A. Li (Jinan University) for molecular assays; and Y. Bai (Peking University Shenzhen Graduate School) for the technique of calcium imaging. **Funding:** This study was supported by National Key Research and Development Program of China (2016YFC1306702) to K.-F.S. and L.Z., National Natural Science Foundation of China (31500842 and 81771455) to L.Z. and K.-F.S., respectively, and Guangdong Natural Science Foundation (2016A030313082) to L.Z. **Author contributions:** K.C. and L.Z. designed the research plan. K.C., Y.Z., J.-a.W., and H.O. performed all experiments. X.H. performed electrophysiological recordings. F.Z. participated in the calcium recording assay. L.Z. and K.C. wrote the manuscript. K.-F.S., C.S.W.L., and C.R. revised the manuscript. L.Z. and K.-F.S. supervised all experiments. **Competing interests:** The authors declare that they have no competing interests. **Data and materials availability:** All data needed to evaluate the paper are present in the paper and/or the Supplementary Materials. Additional data related to this paper may be requested from the corresponding authors.

Submitted 27 November 2018
Accepted 23 May 2019
Published 3 July 2019
10.1126/sciadv.aaw1888

Citation: K. Chen, Y. Zheng, J.-a. Wei, H. Ouyang, X. Huang, F. Zhang, C. S. W. Lai, C. Ren, K.-F. So, L. Zhang, Exercise training improves motor skill learning via selective activation of mTOR. *Sci. Adv.* **5**, eaaw1888 (2019).